The Cryosphere Discuss., https://doi.org/10.5194/tc-2017-227
Manuscript under review for journal The Cryosphere
Discussion started: 20 October 2017

The Cryosphere Discussions
Open Access
EGU

Nitrate deposition and preservation in the snowpack along a traverse from coast to the ice sheet summit (Dome A) in East Antarctica

Guitao Shi[1,2], Meredith G. Hastings[3], Jinhai Yu[2,4], Tianming Ma[2,5], Zhengyi Hu[2], Chunlei An[1], Chuanjin Li[6], Hongmei Ma[2], Su Jiang[2], and Yuansheng Li[2]

[1] School of Geographic Sciences, East China Normal University, Shanghai 200241, China
[2] Key Laboratory for Polar Science of State Oceanic Administration, Polar Research Institute of China, Shanghai 200062, China
[3] Department of Earth, Environmental and Planetary Sciences and Institute at Brown for Environment and Society, Brown University, Providence, Rhode Island 02912, USA.
[4] School of Geographic and Oceanographic Sciences, Nanjing University, Nanjing 210023, China
[5] School of Ocean and Earth Science, Tongji University, Shanghai 200092, China
[6] The State Key Laboratory of the Cryospheric Sciences, Northwest Institute of Eco-Environment and Resources, Chinese Academy of Sciences, Lanzhou 730000, China

Correspondence to: G. Shi (gt_shi@163.com) and M.G. Hastings (meredith_hastings@brown.edu)

The Cryosphere Discuss., https://doi.org/10.5194/tc-2017-227
Manuscript under review for journal The Cryosphere
Discussion started: 20 October 2017

Abstract. The Antarctic ice core nitrate (NO_3^-) can provide a unique record of the atmospheric reactive nitrogen cycle. However, the factors influencing the deposition and preservation of NO_3^- at the ice sheet surface must first be understood. Therefore, an intensive program of snow sample collections was made on a traverse from the coast to the ice sheet summit, Dome A, East Antarctica. Snow samples in this observation include 120 surface snow samples (top ~3cm), 20 snowpits with depths of 150 to 300cm, and 6 crystal ice samples (the topmost needle like layer on Dome A plateau), and NO_3^- concentrations in these samples were determined. The main purpose of this investigation is to characterize the distribution pattern and preservation of NO_3^- in the snow in different environments. Results show that an increasing trend of NO_3^- concentrations with distance inland is present in surface snow, and NO_3^- is extremely enriched in the crystal ice (with a maximum of 16.1 μeq L^{-1}). NO_3^- concentration profiles for snowpits vary between coastal and inland sites. On the coast, the deposited NO_3^- was largely preserved, and the archived NO_3^- fluxes are dominated by snow accumulation. The relationship between the archived NO_3^- and snow accumulation rate can be well depicted by a linear model, suggesting a homogeneity of atmospheric NO_3^- levels. It is estimated that dry deposition contributes 27-44 % of the archived NO_3^- fluxes, and the dry deposition velocity and scavenging ratio for NO_3^- was relatively constant near the coast. Compared to the coast, the inland snow shows a relatively weak association between archived NO_3^- and snow accumulation, and the archived NO_3^- fluxes were more concentration dependent. The association between NO_3^- and the coexisting ions ($nssSO_4^{2-}$, Na^+ and Cl^-) was assessed, and $nssSO_4^{2-}$ (the fine aerosol particles) could potentially influence NO_3^- concentrations, while the correlation between NO_3^- and Na^+ (mainly associated with coarse aerosol particles) is not significant. In inland snow, there were no significant relationships found between NO_3^- and the coexisting ions, suggesting a dominant role of NO_3^- recycling in the concentration.

The Cryosphere Discuss., https://doi.org/10.5194/tc-2017-227
Manuscript under review for journal The Cryosphere
Discussion started: 20 October 2017

1 Introduction

As the major sink of atmospheric nitrogen oxides (NO_x= NO and NO_2), nitrate (NO_3^-) is one of the major chemical species measured in polar snow and ice. The measurements of NO_3^- in ice cores may offer potential for understanding the complex atmospheric nitrogen cycle as well as oxidative capacity of the atmosphere through time (Legrand and Mayewski, 1997; Alexander et al., 2004; Hastings et al., 2009; Geng et al., 2017). However, the sources, transported pathways, and preservation of NO_3^- are still not well understood in Antarctic snowpack, hampering the interpretation of ice core NO_3^- records.

The accumulation of NO_3^- in snow is associated with various environmental factors and continental, atmospheric and stratospheric sources could influence NO_3^- concentrations (Wolff, 1995; McCabe et al., 2007; Wolff et al., 2008; Lee et al., 2014). In surface snow, NO_3^- levels are thought to be linked with snow accumulation rate, and higher values are usually present in areas with low accumulation, e.g., East Antarctic plateaus (Qin et al., 1992; Erbland et al., 2013; Traversi et al., 2017). Unlike sea salt related ions (e.g., chloride (Cl^-), sodium (Na^+), and occasionally sulfate (SO_4^{2-})), NO_3^- does not usually show an elevated level in coastal Antarctic snow (Mulvaney and Wolff, 1994; Bertler et al., 2005; Frey et al., 2009), suggesting a negligible contribution from sea salt aerosol. However, the marine emissions of alkyl NO_3^-, particularly methyl and ethyl NO_3^-, produced in surface oceans by microbiological and/or photochemical processes, are thought to be a possible contribution to Antarctic NO_3^- (Jones et al., 1999; Liss et al., 2004).

The anthropogenic contribution, so far, is negligible in Antarctica while industrial and/or agricultural emissions have contributed to increasing NO_3^- levels in Greenland snow and ice over recent decades to hundreds of years (Mayewski and Legrand, 1990; Hastings et al., 2009; Felix and Elliott, 2013; Geng et al., 2014). Recently, adjoint model simulations proposed that tropospheric transport of NO_3^- from the mid-low latitudes is an important source of Antarctic NO_3^- year round, though less so in austral spring/summer (Lee et al., 2014). A recent treatment of NO_3^- in snow in the same global chemical transport model suggests that the recycling of NO_3^- and/or transport of NO_x due to photolysis of NO_3^- in the surface snow layer is likely important in summertime (Zatko et al., 2016). The stratospheric inputs of NO_3^- via polar stratospheric cloud (PSC) sedimentation is also thought to be an important origin of Antarctic NO_3^-, and this source has been used to explain the sporadic NO_3^- concentration spikes in later winter and/or spring (Wagenbach et al., 1998; Savarino et al., 2007; Traversi et al., 2017). At some sites, the snow/ice core NO_3^- concentrations were found to be linked with regional atmospheric circulation (e.g., sea level pressure gradient;(Goodwin et al., 2003; Russell et al., 2006). In general, atmospheric circulation appears not to affect snow NO_3^- concentrations directly, but indirectly through an influence on the air mass transport and/or snow accumulation rate (Russell et al., 2004; Russell et al., 2006). In addition, Antarctic snow/ice NO_3^- is also thought to be linked with extraterrestrial fluxes of energetic particles and solar irradiation, and it has been reported that solar flares can lead to significant NO_3^- spikes in polar ice (Zeller et al., 1986; Traversi et al., 2012). However, there are also investigations suggesting that there is not necessarily a connection between solar variability and snow NO_3^- concentrations (Mosley-Thompson et al., 1991; Wolff et al., 2008). In summary, factors influencing NO_3^- levels in snow/ice are complicated, and the significance of the relationship between NO_3^- and controlling factors may be temporally and spatially dependent.

After deposition, NO_3^- can be altered via post-depositional processes, and ultraviolet photolysis and possibly volatilization are thought to be the main processes of NO_3^- loss (Frey et al., 2009; Erbland et al., 2013; Berhanu et al., 2015). In snowpack, the solar radiation decreases exponentially, with

attenuation described in terms of an *e*-folding depth (z_e) where the actinic flux is reduced to 37 % (i.e. 1/*e*) of the surface value. Thus, about 95 % of snowpack photochemistry is expected to occur above the depth of three times z_e (Warren et al., 2006). At remote Antarctic sites, the z_e is calculated to be about 20 cm, and this depth is dependent upon the concentration of impurities contained in the snow (Zatko et al., 2013). The effects of volatilization of NO_3^- are currently in debate, and a field experiment suggests that this process is an active player in NO_3^- loss (Erbland et al., 2013), while laboratory studies show that volatilization of NO_3^- is negligible (Cragin and McGilvary, 1995; Sato et al., 2008). Further investigations are needed to examine the potential effects of this process, for a better understanding of post-depositional processing of NO_3^- in the snow. Based on z_e, NO_3^- at deeper depths in Antarctic snow (e.g., > 100 cm), well beyond the snow photic zone, may be taken as the archived fraction. Thus, NO_3^- in deeper snow possibly provides an opportunity to investigate the archived fraction and potential influencing factors (e.g., snow accumulation rate). Given that an extensive array of ice core measurements is unavailable in most of Antarctica, the deeper snowpits (with depth > 100 cm) may offer a useful way to investigate the archived NO_3^- (Shi et al., 2015).

To date, investigations on spatial and temporal patterns of snow NO_3^- have been performed on several traverses in Antarctica (e.g., 1990 International Trans-Antarctica Expedition, and DDU to Dome C; Qin et al., 1992; Frey et al., 2009; Erbland et al., 2013), but these provide an uneven distribution of snow NO_3^- concentrations, leaving large regions un-sampled (e.g., Lambert Glacier basin and Dome A plateau). Over the past few decades, while several glaciological observations have been carried out on the Chinese inland Antarctic traverse route from Zhongshan to Dome A, East Antarctica (Hou et al., 2007; Ding et al., 2010; Ma et al., 2010; Ding et al., 2011; Li et al., 2013), detailed data on snow chemistry are still rare, especially detailed information on NO_3^-. From 2009 to 2013, we therefore conducted surface snow and snowpit sampling campaigns along the traverse route, and the main objectives were (1) to describe NO_3^- distribution in surface snow and snowpits, (2) to characterize the association between archived NO_3^- and snow accumulation rate, and (3) to examine the potential effects of coexisting ions on NO_3^- preservation. The results of this study may help to better understand NO_3^- deposition and preservation in the snowpack, which is critical to the interpretation of ice core NO_3^- records.

2 Methodology

2.1 Study area (Zhongshan to Dome A traverse)

The Zhongshan to Dome A CHINARE (Chinese National Antarctic Research Expedition) inland traverse is an important leg of the ITASE (International Trans-Antarctic Scientific Expedition). The traverse is in the Indian Ocean sector of East Antarctica, passing through the Lambert Glacier, the largest glacier in Antarctica. In January 1997 the first Chinese Antarctic inland expedition reached an area ~300 km from the coast; in January 1998 the traverse was extended to 464 km, and in December 1998, to the Dome A area ~1100 km from the coast. In the austral 2004/2005 summer for the first time, the traverse extended to the ice sheet summit, Dome A, a total distance of ~1260 km. In January 2009, the Chinese inland research base, Kunlun Station, was established at Dome A, mainly aiming at deep ice core drilling and astronomical observations. Now, Kunlun base is a summer station, and the CHINARE team typically conducts an annual inland traverse from the coastal Zhongshan station to Dome A.

In January 2010, the Dome A deep ice core project was started, and the construction of basic

infrastructure (including drill trench and scientific workroom) cost 4 summer seasons. The deep ice core drilling began in January 2013, and in total 801 m ice core was recovered by 2016/2017 season. The investigation of NO_3^- deposition and preservation in the snowpack will be of help to the interpretation of Dome A deep ice core NO_3^- records.

2.2 Sample collection

During the 2010/2011 CHINARE, surface snow samples (the topmost ~3 cm) were collected at an interval of ~10 km along the traverse route from Zhongshan to Dome A, using 3.0 cm diameter high-density polyethylene (HDPE) bottles (volume = 100 ml). The bottles were pre-cleaned with Milli-Q ultrapure water (18.2 MΩ), until electrical conductivity of the water stored in bottles (> 24 h) decreased to <0.5 μS cm^{-1}. Then, the bottles were dried under a class 100 super clean hood at 20 ^oC. Immediately after the drying procedure, the bottles were sealed in clean PE bags that were not opened until the field sampling started. At each sampling site (typically > 500 m away from the traverse route), the bottles were pushed into surface snow layers in the windward direction. In total, 120 surface snow samples were collected. In addition, at each sampling site, the upper snow density (~10 cm) was measured using a density scoop with the volume of 1000 cm^3. Pre-cleaned bottles filled with Milli-Q water taken to the field and treated to the same conditions as field samples to represent field blanks (n = 3).

On the Dome A plateau, the snow is soft and non-cohesive, and morphology of the surface snow is different from other areas on the traverse, with a needle ice crystal layer extensively developed, especially on the sastrugi (Fig. S1 in supporting information). The depth of the needle-like crystal ice layer (referred to as the "crystal ice" in the following context) is generally < 1.0 cm. In order to investigate air-snow transfer of NO_3^- in this uppermost ~1 cm layer, the crystal ice was collected using a clean HDPE scoop, and then was poured into the clean wide mouth HDPE bottles. Approximately 30 g of crystal ice was collected for each sample. In total, 6 crystal ice samples were collected on the traverse near Dome A plateau.

In addition to surface snow, snowpit samples were collected during CHINARE inland traverse campaigns in 2009/2010, 2010/2011, and 2012/2013. The snowpits were excavated manually, and the snow wall in the windward direction was scraped clean and flat with a clean HDPE scraper. Then the bottles were pushed horizontally into the snow wall. Snowpit samples were collected from the base towards the top layer along a vertical line. During the sampling process, all personnel wore PE gloves and facemasks to minimize potential contamination. Note that the snowpits are generally > 1 km from the traverse route to also avoid possible contamination from the expedition activities. The full information about individual snowpits, including location, distance from the coast, elevation, snowpit depth, sampling resolution, collection date, and annual snow accumulation rate, is summarized in Table 1. All together, 20 snowpits, 1741 snow samples, were collected.

After snow collection, the bottles were sealed in clean PE bags again and preserved in clean thermal insulated boxes. All of the samples were transported to the laboratory under freezing conditions (< -20 ^oC).

2.3 Sample analysis

Snow samples were melted in the closed sampling bottles on a super clean bench (class 100) before chemical measurements. Analyses of Na^+, NH_4^+, K^+, Mg^{2+}, Ca^{2+}, Cl^-, NO_3^- and SO_4^{2-} were performed using a Dionex ICS-3000 ion chromatography system. The column used for cation analysis (Na^+, NH_4^+,

178 K^+, Mg^{2+} and Ca^{2+}) was a Dionex column CS12 (2×250 mm), with a guard column CG12 (2×50 mm);
179 while the anions (Cl^-, NO_3^- and SO_4^{2-}) were analyzed using a Dionex column AS11 (2×250 mm) with a
180 guard column AG11 (2×50 mm). The eluent for cations was 18.0 mM methanesulfonic acid (MSA),
181 and the gradient elution method was employed for anion analysis, with eluent of potassium hydroxide
182 (KOH). More details on this method are described in a previous report (Shi et al., 2012). During sample
183 analysis, duplicated samples and field blanks were synchronously analyzed. The pooled standard
184 deviation (σ_p, $\sigma_p = \sqrt{\sum_{i=1}^{k}(n_i-1)s_i^2 / \sum_{i=1}^{k}(n_i-1)}$, where n_i and s_i^2 are the size and variance of the
185 *i*th samples respectively, and k is the total number of sample sets) of all replicate samples run at least
186 twice in two different sample sets is 0.019 (Cl^-), 0.023 (NO_3^-), 0.037 (SO_4^{2-}), 0.022 (Na^+), 0.039 (NH_4^+),
187 0.006 (K^+), 0.006 (Mg^{2+}) and 0.006 (Ca^{2+}) μeq L^{-1} respectively (n = 65 pairs of samples). Ion
188 concentrations in field blanks (n = 9) are generally lower than the detection limit (DL, 3 standard
189 deviations of water blank in the laboratory).
190 For Antarctic snow samples, the concentrations of H^+ are usually not measured directly, but deduced
191 from the ion-balance disequilibrium in the snow. Here, H^+ concentration is calculated as follows
192 (Legrand and Delmas, 1988).
193 $[H^+] = [SO_4^{2-}] - 0.12 \times [Na^+] + [NO_3^-] + [Cl^-] - 1.17 \times [Na^+]$ (Eq. 1),
194 where ion concentrations are in μeq L^{-1}. In addition, the non-sea-salt fractions of SO_4^{2-} ($nssSO_4^{2-}$) and
195 Cl^- ($nssCl^-$) can be calculated from the following expressions, by assuming Na^+ exclusively from sea
196 salt (in μeq L^{-1}).
197 $[nssSO_4^{2-}] = [SO_4^{2-}] - 0.12 \times [Na^+]$ (Eq. 2),
198 $[nssCl^-] = [Cl^-] - 1.17 \times [Na^+]$ (Eq. 3).
199
200 **3 Results**
201
202 **3.1 NO_3^- concentration in surface snow**
203 Concentrations of NO_3^- in surface snow are shown in Fig. 1, ranging from 0.6 to 5.1 μeq L^{-1}, with a
204 mean of 2.4 μeq L^{-1}. One standard deviation (1σ) of NO_3^- concentration in surface snow is 1.1 μeq L^{-1},
205 with *Cv* (1σ over mean) of 0.5, indicating a moderate spatial variability. On the coastal ~450 km, NO_3^-
206 shows a slightly increasing trend towards the interior, with a low variability, while NO_3^- concentrations
207 are higher in the inland region, with a large fluctuation. It is notable that in the area ~800 km from the
208 coast, where snow accumulation is relatively high, NO_3^- concentrations decrease to < 2.0 μeq L^{-1},
209 comparable to the values on the coast. Near the Dome A plateau (> 1000 km from coast), there is a
210 tendency for higher NO_3^- concentrations (> 5.0 μeq L^{-1}).
211 The percentage that surface snow NO_3^- contributes to total ions (i.e., total ionic strength, sum of Na^+,
212 NH_4^+, K^+, Mg^{2+}, Ca^{2+}, Cl^-, NO_3^-, SO_4^{2-} and H^+, in μeq L^{-1}) varies from 6.7 to 37.6 % (mean = 24.6 %),
213 with low values near the coast and high percentages on the plateau. A strong relationship was found
214 between NO_3^- and the total ionic strength in surface snow (r = 0.74, p < 0.01).
215 In terms of crystal ice, NO_3^- concentrations range from 8.4 to 16.1 μeq L^{-1} (mean = 10.4 μeq L^{-1}),
216 significantly higher than those of surface snow (independent samples t test, p<0.01; Fig. 1). In the
217 crystal ice, the percentage of NO_3^- accounting for the total ions is 38-42 %, higher than the values of
218 surface snow. In general, NO_3^- concentrations in crystal ice are comparable to the values of the top 0.4
219 cm snow layer at Dome C (9 – 22 μeq L^{-1} in summertime;(Erbland et al., 2013). If H^+ is excluded for
220 the calculation of total ionic strength in crystal ice, the percent increases to 72-80 %. In addition, a

significant correlation was found between NO_3^- and the total ionic strength in crystal ice (r = 0.99, p < 0.01).

NO_3^- concentrations in surface snow have been widely measured across Antarctica (Fig. 2), and the values vary from 0.2 to 12.9 μeq L^{-1}, with a mean of 2.1 μeq L^{-1} (n = 594, 1σ = 1.7 μeq L^{-1}) and a median of 1.4 μeq L^{-1}. Most of the data (87 %) fall in the range of 0.5 - 4.0 μeq L^{-1}, and only 7 % of the values are above 5.0 μeq L^{-1}, mainly on the East Antarctic plateau. Spatially, NO_3^- concentrations show an increasing trend with distance inland, and the values are higher in East than in West Antarctica. Overall, this spatial pattern is opposite to that of the annual snow accumulation rate (Arthern et al., 2006), i.e., low (high) snow accumulation corresponds to high (low) NO_3^- concentrations. It is difficult to compare with NO_3^- concentrations derived from the "upper snow layer" in different studies because each study sampled a different depth (Fig. 2), e.g., 10 cm for DDU-Dome C traverse (Frey et al., 2009), 25 cm for the 1989-90 International Trans-Antarctica Expedition (Qin et al., 1992) and 3 cm for this study. The different sampling depths appears to result in large differences in NO_3^- concentration, especially on the East Antarctic plateaus (e.g., the values of the topmost 1 cm of snow, the crystal ice, can be up to >15 μeq L^{-1}; Fig. 1). In this case, any comparison of NO_3^- concentrations in surface snow collected in different campaigns should be made with caution.

3.2 Snowpit NO_3^- concentrations

Mean NO_3^- concentrations for snowpits are shown in Fig. 1. On the coastal ~450 km, snowpit NO_3^- means are comparable to those of surface snow; whereas, NO_3^- means are lower in inland snowpits than in surface snow with the exception of sites ~800 km from the coast. In general, the differences between snowpit NO_3^- means and the corresponding surface snow values are small at sites with high snow accumulation (e.g., close to coast), while the differences are large in low snow accumulation areas (e.g., near Dome A).

The profiles of NO_3^- for all snowpits are shown in Fig. 3. NO_3^- concentrations vary remarkably with depth in pits SP1 - SP5, which are located near the coast. Although SP2 and SP5 show high NO_3^- concentrations in the topmost sample, the data from deeper depths can be compared with the surface values. In addition, NO_3^- means for the entire snowpits are close to the means of the topmost layer covering a full annual cycle of accumulation (i.e., the most recent year of snow accumulation) at SP1-SP5 (Fig. 4). Given the high snow accumulation (Fig. 1), NO_3^- variability in coastal snowpits is likely suggestive of a seasonal signature (Wagenbach et al., 1998; Grannas et al., 2007; Shi et al., 2015).

In contrast, most of the inland snowpits show high NO_3^- concentrations in the top layer, and then fall sharply from > 2.0 μeq L^{-1} in top snow to < 0.2 μeq L^{-1} in the first meter of depth (Fig. 3). NO_3^- means for the entire snowpits are typically lower than those of the most recent one-year snow layer (Fig. 4). Similar NO_3^- profiles for snowpits have been reported elsewhere in Antarctica, maybe resulted from post-depositional processing of NO_3^- (Röthlisberger et al., 2000; McCabe et al., 2007; Erbland et al., 2013; Shi et al., 2015).

Comparison of the NO_3^- profile patterns reveals significant spatial heterogeneity, even for neighboring sites. For instance, sites SP11 and SP12, 14 km apart, feature similar snow accumulation rate (Table 1). If it is assumed that snow accumulation is relatively constant during the past several years at SP11 (sampled in 2012/2013), snow in the depth of ~54 cm corresponds to the deposition in 2009/2010 (snow density = 0.45 g cm^{-3}, from field measurements). NO_3^- concentrations are much higher in the top snow of SP12 (sampled in 2009/2010) than in the depth of ~54 cm in SP11 (Fig. 3).

The Cryosphere Discuss., https://doi.org/10.5194/tc-2017-227
Manuscript under review for journal The Cryosphere
Discussion started: 20 October 2017

This variation in NO_3^- profiles at a local scale has been reported, possibly related to local morphologies associated with sastrugi formation and wind drift (Frey et al., 2009; Traversi et al., 2009). It is interesting that higher NO_3^- concentrations were not found in the uppermost layer at sites SP7 and SP8 (~600 km from coast; Fig. 3), where large sastrugi with hard smooth surfaces was extensively developed (from field observations; Fig. S2). Snow accumulation rate in this area fluctuates remarkably, and the values of some sites are rather small or close to zero due to the strong wind scouring (Fig. 1) (Ding et al., 2011; Das et al., 2013). In this case, the snowpit NO_3^- profiles appear to be largely influenced by wind scour on snow, possibly resulting in missing years and/or intra-annual mixing.

4 Discussion

4.1 Accumulation influence on NO_3^-

The preservation of NO_3^- is thought to be closely associated with snow accumulation, where most of the deposited NO_3^- is preserved at sites with higher snow accumulation (Wagenbach et al., 1994; Hastings et al., 2004; Fibiger et al., 2013). Whereas, NO_3^- may be altered significantly at sites with low snow accumulation (Blunier et al., 2005; Grannas et al., 2007; Frey et al., 2009; Erbland et al., 2013). In the following discussion, we divide the traverse into two zones, i.e., the coastal zone (~<450 km from the coast, including SP1-SP5 and Core 1; Table 1) and the inland region (~450 km to Dome A, including pits SP6-SP20 and Core 2; Table 1), following NO_3^- distribution patterns in surface snow and snowpits (sections 3.1 and 3.2) as well as the spatial pattern of snow accumulation rate (Fig. 1).

As for snowpits, NO_3^- levels in top and deeper layers are comparable near the coast, while NO_3^- differs considerably between the upper and deeper snow at inland sites (Figs. 3 and 4). It is proposed that photochemical processing is responsible for NO_3^- distribution in inland snowpits (Erbland et al., 2013; Berhanu et al., 2015). Considering that the actinic flux is always negligible below the depth of 1 m (Zatko et al., 2013), the bottom layers of the snowpits (i.e., > 100 cm; Table 1) are well below the photochemically active zone. In this case, NO_3^- in the bottom snowpit can be taken as the archived fraction. Here, we define NO_3^- in the bottom layer covering a full annual cycle of deposition as an approximation of the annual mean of preserved NO_3^- (i.e., beyond photochemical processing; denoted as "p-concentration" in the following context; Fig. 4), thus allowing for calculating the archived annual NO_3^- flux (i.e., the product of p-concentration and annual snow accumulation rate). Although there is uncertainty over the calculation of archived NO_3^- flux due to interannual variability in NO_3^- inputs and snow accumulation, this assumption provides a useful way to investigate the relationship between preservation of NO_3^- and physical factors considering that an extensive array of ice core measurements is unavailable in most of Antarctica. It is noted that p-concentration is generally close to (lower than) the NO_3^- means for entire snowpits in coastal (inland) Antarctica (Fig. 4).

4.1.1 NO_3^- in coastal snowpack

If it is assumed that atmospheric NO_3^- aerosol levels and dry deposition are similar at various sites, the linear relation between concentration and inverse accumulation can present information about fresh snowfall NO_3^- levels and dry deposition fluxes, interpreted as the following model (Fischer and Wagenbach, 1996).

$$C_{firn} = F(NO_3^-) \times 1/A + C_{f\text{-}snow} \quad \text{(Eq. 4)},$$

where C_{firn} is measured firn NO_3^- concentration, here taking $C_{firn} \approx$ p-concentration of NO_3^-; $F(NO_3^-)$ is annual dry deposition flux of NO_3^-; A is annual snow accumulation rate; and $C_{f\text{-}snow}$ is NO_3^-

concentration in fresh snowfall. A strong relationship of C_{firn} vs. $1/A$ suggests spatial homogeneity of fresh snow NO_3^- levels and dry deposition flux, and a weak correlation implies a variable condition. Figure 5a shows that p-concentration is closely related to snow accumulation on the coast ($r^2 = 0.95$), and a very strong linear relationship was found between p-concentration of NO_3^- and $1/A$ for coastal snowpits (Fig. 5b), suggesting that fresh snow concentration and dry deposition flux of NO_3^- are spatially homogeneous on the coast. The intercept and slope of the linear fit suggest a NO_3^- concentration in fresh snow and a NO_3^- dry deposition flux of 0.7±0.07 μeq L^{-1} and 45.7±7.8 μeq m^{-2} a^{-1} respectively.

Figure 5c shows the archived fluxes of NO_3^- on the coast, with values from 104 (at the lowest accumulation site) to 169 μeq m^{-2} a^{-1} (at the highest accumulation site). The strong relationship between NO_3^- flux and snow accumulation suggests that wet deposition dominates the archived NO_3^- flux. Taking the calculated NO_3^- dry deposition flux of 45.7 μeq m^{-2} a^{-1}, dry deposition accounts for 27-44 % (mean = 36 %) of total NO_3^- inputs, with higher (lower) percentages at lower (higher) snow accumulation sites. This result is consistent with the observations in Taylor Valley (coastal West Antarctica), where the snowfall was found to be the primary driver for NO_3^- inputs (Witherow et al., 2006). This result is also generally consistent with, but greater than that in the modeling study of Zatko et al. (2016), which predicts a ratio of dry deposition to total deposition of NO_3^- in Antarctica as < 20 % close to the coast, increasing towards the plateaus.

Alley et al. (1995) proposed a model describing the relationship among snow NO_3^- flux (F_{total}) and atmospheric concentration of NO_3^- (C_{atm}) and snow accumulation rate (A), where::

$$F_{total} = K_1 C_{atm} + K_2 C_{atm} A \text{ (Eq. 5)},$$

$$F_{total} = C_{firn} \times A \text{ (Eq. 6)},$$

where K_1 is the dry deposition velocity (cm s^{-1}); dimensionless K_2 is the scavenging ratio for precipitation; and C_{firn} is the same as that in Eq 4. If K_1 and K_2 are constants, a straight line would be expected between total flux and snow accumulation, with the intercept $K_1 C_{atm}$ being an approximation of dry deposition rate. So, NO_3^- flux vs. accumulation fitting a simple straight line (Fig. 5c) suggests that K_1 and K_2 are relatively constant on the coast, and the dry deposition flux value (50.3±8.1 μeq m^{-2} a^{-1}) is comparable to that yielded from Eq. 4 (45.7±7.8 μeq m^{-2} a^{-1}). Both model results support that NO_3^- dry deposition is homogeneous on the coast. If taking C_{atm}= 20.9±5.3 ng m^{-3} near the coast (unpublished data), K_1 is estimated to be 0.5 cm s^{-1}, identical to a typical estimate for HNO_3 deposition velocity to a snow/ice surface (0.5 cm s^{-1};(Seinfeld and Pandis, 1997). This predicted K_1 value also compares well to that estimated at South Pole (0.8 cm s^{-1}). The scavenging ratio for NO_3^- (K_2) is estimated to be 0.2×10^4, much lower than the values at high alpine sites where the coarse aerosol particles are predominant (Kasper-Giebl et al., 1999), but comparable to the numbers in eastern Canada (~2000;(Barrie, 1985). The scavenging ratio for NO_3^- (K_2) can also be calculated from the following expression (Kasper-Giebl et al., 1999),

$$K_2 = \rho_{atm} \times (C_{f\text{-}snow} / C_{atm}) \text{ (Eq. 7)},$$

where ρ_{atm} is air density (g m^{-3}), and $C_{f\text{-}snow}$ and C_{atm} are NO_3^- concentrations in fresh snow (ng g^{-1}) and atmosphere (ng m^{-3}) respectively. If taking $\rho_{atm} \approx 1.0$ kg m^{-3} (the average ground surface temperature $t \approx$ 255 k, and ground pressure $P \approx 0.08$ MPa near the coast), $C_{f\text{-}snow}$ = 43 ng g^{-1} (see discussion above and section 4.2 below), and C_{atm}= 20.9±5.3 ng m^{-3}, K_2 is calculated to be ~2100, comparable to the linear model prediction (Eq. 5). These parameters inferred from the observations provide useful reference values for modeling NO_3^- recycling in Antarctica.

Figure 5d shows the distribution of flux is negatively tied to p-concentration of NO_3^-, which is not

353 surprising since p-concentration is negatively related to accumulation. Based on the regression analysis
354 (Figs. 5c and d), the archived NO_3^- flux is more accumulation dependent compared to the concentration.
355 This is compatible with the observations in Greenland (Burkhart et al., 2009), where accumulation is
356 generally above 100 kg m^{-2} a^{-1}.
357 In terms of surface snow on the coast, NO_3^- may be disturbed by the katabatic winds and wind
358 convergence located near the Amery Ice Shelf (that is, the snow-sourced NO_x and NO_3^- from Antarctic
359 plateau possibly contribute to coastal snow NO_3^-) (Parish and Bromwich, 2007; Ma et al., 2010). In
360 addition, the sampled ~3 cm surface layer roughly corresponds to the net accumulation in the past
361 0.5-1.5 months assuming an even distribution of snow accumulation in the course of a single year. This
362 difference in exposure time of the surface snow at different sampling sites, could possibly affect the
363 concentration of NO_3^-, although the post-depositional alteration of NO_3^- was thought to be minor on the
364 coast (Wolff et al., 2008; Erbland et al., 2013; Shi et al., 2015). Taken together, NO_3^- in coastal surface
365 snow might represent some post-depositional alteration. Even so, a negative association between NO_3^-
366 concentration and snow accumulation was found at the coast (Figs. 6a and b), suggesting that overall
367 the majority of the NO_3^- appears to be preserved and is driven by snow accumulation.
368
369 **4.1.2 NO_3^- in inland snowpack**
370 In comparison with the coast, the association between p-concentration and snow accumulation is
371 relatively weak in inland Antarctica (Figs. 5e and f), suggesting more variable conditions in ambient
372 concentrations and dry deposition flux of NO_3^-. In addition, the relationship of p-concentration vs.
373 (inverse) accumulation in inland is opposite to that of coast. Based on current understanding of the
374 post-depositional processing of NO_3^-, the negative correlation between p-concentration and inverse
375 snow accumulation (Fig. 5f) possibly suggests a loss of NO_3^- owing to photolysis and/or volatilization.
376 A similar relationship has also been documented in Dronning Maud Land (DML, with snow
377 accumulation of 27-70 kg m^{-2} a^{-1}), where NO_3^- concentrations are strongly correlated with snow
378 accumulation ($r^2 > 0.9$) (Pasteris et al., 2014). The difference in the relationship strength (NO_3^- vs.
379 accumulation) between DML and this study is possibly related with the relatively small variability of
380 accumulation in DML (vs. inland region under very varied conditions; Fig. 1).
381 The archived NO_3^- fluxes vary considerably among inland sites, from ~3 to 333 μeq m^{-2} a^{-1}, with
382 high values generally corresponding to high snow accumulation, similar to coastal results (compare
383 Figs. 5c and g). However, the nearly 1:1 relationship between p-concentration and NO_3^- flux (Fig. 5h),
384 suggests that accumulation rate is not the main driver of the preserved NO_3^- concentration. In inland
385 Antarctica, the archived NO_3^- fraction is largely influenced by the length of time that NO_3^- was exposed
386 to UV radiation (Berhanu et al., 2015), which decreases exponentially in the snowpack. The *e*-folding
387 depth, z_e value, is thought to be influenced by a variety of factors, such as co-existent impurities (e.g.,
388 black carbon), bulk density and grain size (Zatko et al., 2013). In addition, the snow albedo is also
389 dependent on snow physical properties (Carmagnola et al., 2013). Taken together, this suggests that the
390 inland plateau is below a "threshold" of accumulation rate such that the archived NO_3^- flux cannot be
391 explained by snow accumulation rate.
392 Among the inland sites, it is noted that SP10 and Core2 (~800 km from the coast), featured by high
393 snow accumulation rate (> 100 kg m^{-2} a^{-1}; Table 1 and Fig. 1), exhibit higher values of p-concentration
394 and archived fluxes of NO_3^- than those of the coastal sites. The high concentration and flux values near
395 the two sites may be associated with NO_3^- recycling driven by photolysis (Frey et al., 2009; Zatko et al.,
396 2016), but this speculation should be tested further (e.g., studying the isotopes of NO_3^-).

The inland region is generally characterized with low accumulation (<55 kg m^{-2} a^{-1}; Fig. 1). At these sites, snow NO_3^- is more likely to undergo post-depositional alteration, e.g., a severe loss of NO_3^- (Frey et al., 2009; Zatko et al., 2016). During photolysis, the lost NO_3^- can be recycled in the local environment, i.e., re-formed NO_3^- from photoproducts can be re-deposited, resulting in concentrated NO_3^- in surface snow (Erbland et al., 2013). It appears that the high NO_3^- concentrations in inland surface snow and crystal ice near Dome A (Fig. 1) can be explained by this mechanism. Thus far, several modeling works have been performed to understand NO_3^- recycling processes across Antarctica (e.g.,(Erbland et al., 2015; Zatko et al., 2016), however, much uncertainty remains about NO_3^- recycling and preservation. It is thought that emission and transport strength are the factors controlling the recycling of NO_3^-, while the former is associated with initial NO_3^- concentrations, UV and snow accumulation, and the latter is linked with air mass movement (Wolff et al., 2008; Frey et al., 2009). As a result, snow accumulation alone is insufficient to explain NO_3^- variability in the surface snow (i.e., no significant correlation between NO_3^- concentration and snow accumulation; Figs. 6c and d).

4.2 Effects of coexisting ions on NO_3^-

Atmospheric NO_3^- in Antarctica is thought to be mainly associated with mid-latitude sources, re-formed NO_3^- driven by snow-sourced photolysis products, and/or stratospheric inputs (Savarino et al., 2007; Lee et al., 2014; Traversi et al., 2017). We investigate whether NO_3^- in snow is closely associated with coexisting ions (e.g., Cl^-, SO_4^{2-}, Na^+, K^+, Mg^{2+} and Ca^{2+}) since these ions have different main sources, e.g., Cl^- and Na^+ are predominantly influenced by sea salt, and SO_4^{2-} is likely dominated by marine inputs (e.g., sea salt and bio-activity source) (Bertler et al., 2005). In the snow, Cl^-, Na^+ and SO_4^{2-} are the most abundant ions in addition to NO_3^-, and the potential association between NO_3^- and the three ions is discussed here.

During austral summer, snow $nssSO_4^{2-}$, mainly derived from ocean bioactivities, accounts for 75 - 99 % (mean=95%) of SO_4^{2-} in surface snow. On the coast, high $nssSO_4^{2-}$ levels correspond to elevated NO_3^- concentrations ($r^2 = 0.32$, $p < 0.01$; Fig. 7a). Similarly, a positive correlation of $nssSO_4^{2-}$ vs. NO_3^- was reported for a coastal ice core near DML ($r^2 = 0.31$) (Laluraj et al., 2010), possibly suggesting that NO_3^- is commonly connected to $nssSO_4^{2-}$ in coastal Antarctica. In the atmosphere, $nssSO_4^{2-}$ can form fine aerosol particles, with long atmospheric residence time (Hara et al., 2014), which is thought to promote NO_3^- formation (Brown et al., 2006; Cook and Roscoe, 2009). This speculation appears to be supported by our recent aerosol observations on this traverse (r^2 between atmospheric NO_3^- and $nssSO_4^{2-}$ of 0.36, p<0.01; unpublished data). On the other hand, the presence of $nssSO_4^{2-}$ aerosol may also enhance the direct uptake of gas phase HNO_3 onto the surface, resulting in NO_3^- deposition via aerosol mechanisms. In both cases, a correlation between NO_3^- and $nssSO_4^{2-}$ would be expected. Thus far, the mechanism of $nssSO_4^{2-}$ influencing NO_3^- in the snowpack, however, is still debated, and it cannot be ruled out that $nssSO_4^{2-}$ further affects mobilization of NO_3^- during and/or after crystallization (Legrand and Kirchner, 1990; Wolff, 1995; Röthlisberger et al., 2000). It is noted that no relationship was found between $nssSO_4^{2-}$ and NO_3^- in inland snow (Fig. 7d), possibly due to the strong alteration of NO_3^- during post-depositional processes, as discussed in section 4.1.2.

In comparison with $nssSO_4^{2-}$ aerosol, the sea-salt aerosols (Na^+) are coarser and can be removed preferentially from the atmosphere due to a larger dry deposition velocity. It is thought that NO_3^- scavenging rate by sea-salt particles is similar to the dry deposition rate of NO_3^- (Hara et al., 2005). If the fresh alkaline sea-salt aerosol could preferentially convert the gaseous HNO_3 to aerosol phase, elevated NO_3^- concentrations with Na^+ spikes in snowpack would be expected, and this association has

been reported for Halley station, a coastal location (Wolff et al., 2008). Here, no significant correlation was found between Na^+ and NO_3^- in coastal snow (Fig. 7b). One possibility is that this relationship is offset by other factors such as snow accumulation and coexistence of impurities (e.g., $nssSO_4^{2-}$), and changes in one or more of these parameters do not always result in a clear relationship between NO_3^- and Na^+ in snowpack. On the other hand, it is possible that the coarse particles are less influential on NO_3^- scavenging, compared to the fine aerosol.

The concentration profiles of NO_3^- and Na^+ in coastal surface snow are shown in Fig. 8, and NO_3^- roughly corresponds to Na^+ in some areas, e.g., 50-150 km and 300-450 km distance inland, although the relation seems not so strong. It is noted that among the 4 snow samples with Na^+ > 1.5 μeq L^{-1} (open circles in Fig. 8), only one sample exhibits NO_3^- spike. This is different from observation at Halley station, where Na^+ peaks usually led to elevated NO_3^- levels in surface snow (Wolff et al., 2008). Of the 4 largest Na^+ spikes, one is fresh snowfall sample (dashed ellipse in Fig. 8), and this sample shows the highest Na^+ concentration (2.8 μeq L^{-1}) and low NO_3^- (0.75 μeq L^{-1}). It is noted that NO_3^- concentration in this fresh snowfall is close to the predictions above (0.7±0.07 μeq L^{-1}; section 4.1.1), validating that the simple linear deposition model (i.e., the Eq. 4) can well depict the deposition and preservation of NO_3^- in coastal snowpack. At inland sites, no association was found between NO_3^- and Na^+ (Fig. 7e), likely explained by the alteration of NO_3^- concentration by post-depositional processing (discussed above).

In surface snow, $nssCl^-$ represents 0-64 % (mean = 40 %) of the total Cl^-. On the coast, it is of interest that $nssCl^-$ in the 4 samples with the highest Na^+ concentrations (open circles in Figs. 7b and 8) are close to 0, and positive $nssCl^-$ values were found for the other samples. Considering the very high Cl^-/Na^+ ratio (mean = 3.1) and the smallest sea ice extent in summertime in East Antarctica (Holland et al., 2014), $nssCl^-$ is unlikely from sea-salt fractionation associated with mirabilite precipitation in sea-ice formation at low temperatures (Marion et al., 1999). In this case, $nssCl^-$ could be mainly related to the deposition of volatile HCl, which is from the reaction of H_2SO_4 and/or HNO_3 with NaCl (Röthlisberger et al., 2003). In other words, the presence of HNO_3 possibly favors the formation of HCl, and this then result in an excess of Cl^- in the snowpack due to emissions and re-deposition of HCl, which could explain the observed relationship between NO_3^- and $nssCl^-$ (Fig. 7c).

With regard to the crystal ice, no significant correlation was found between NO_3^- and the coexisting ions (e.g., Cl^-, Na^+ and SO_4^{2-}), suggesting that these ions are generally less influential on NO_3^- in this uppermost thin layer, compared to the air-snow transfer process of NO_3^- (Erbland et al., 2013). It is noted that NO_3^- accounts for most of the calculated H^+ concentrations (79 - 88 %, mean = 84 %), and a strong linear relationship was found between them (r^2 = 0.99), suggesting that NO_3^- is mainly deposited as acid, HNO_3, rather than in particulate form as salts (e.g., $NaNO_3$ and $Ca(NO_3)_2$). If all of the HNO_3 dissociates to produce H^+ and NO_3^- ions, then the deposition of HNO_3 contributed 76 - 84 % (mean = 80 %) to the total chemical constituents in the crystal ice.

5 Conclusions

Samples of surface snow, snowpits and the uppermost layer of crystal ice, collected on the traverse from the coast to Dome A, East Antarctica, were used to investigate the deposition and preservation of NO_3^- in snow. In general, a spatial trend of NO_3^- in surface snow was found on the traverse, with high (low) concentrations on the plateau (coast). Extremely high NO_3^- levels (e.g., > 10 μeq L^{-1}) were observed in the uppermost crystal ice layer, possibly associated with re-deposition of the recycled NO_3^-. As for the snowpits, NO_3^- exhibits high levels in the top layer and low concentrations at deeper depths

in the inland region, while no clear trend was found on the coast.

On the coast, the archived NO_3^- flux in snow is positively correlated with snow accumulation rate, but negatively with NO_3^- concentration. A linear model can well depict the relationship between archived NO_3^- and snow accumulation, suggesting that atmospheric levels and dry deposition fluxes of NO_3^- are spatially homogeneous on the coast, and the dry deposition plays a minor role in snow NO_3^- inputs. The dry deposition velocity and scavenging ratio for NO_3^- are estimated to be 0.5 cm s^{-1} and 0.2×10^4 respectively. In inland Antarctica, the archived NO_3^- fluxes, varying significantly among sites, are largely dependent on NO_3^- concentration. A weak correlation between snow accumulation and archived NO_3^- suggests variable ambient concentrations and dry deposition flux of NO_3^-, and the relationship is opposite to that for the coast. The post-depositional processing of NO_3^- seems to dominate NO_3^- distribution patterns in surface snow and snowpits in inland Antarctica.

The major ions, Cl^-, SO_4^{2-} and Na^+, originate from different sources from NO_3^-, but could affect the scavenging and preservation of NO_3^-. In coastal surface snow, a positive correlation between $nssSO_4^{2-}$ and NO_3^- possibly supports the presence of fine aerosol favoring NO_3^- formation and scavenging, while the coarse sea salt aerosol (e.g., Na^+) is likely less influential. In contrast to the coast, NO_3^- in inland surface snow is likely dominated by post-depositional processes, and the effects of coexisting ions on NO_3^- appear to be rather minor.

Associated content

Please see the file of Supporting Information.

Acknowledgement

This project was supported by the National Science Foundation of China (Grant nos. 41576190 and 41206188), the International Cooperative Project of the Chinese Arctic and Antarctic Administration (Grant no. 201601), and Chinese Polar Environment Comprehensive Investigation and Assessment Programmes (Grant nos. CHINARE 201X-02-02 and 201X-04-01). We thank the CHINARE inland members for providing help during sampling.

References

Alexander, B., Savarino, J., Kreutz, K.J., and Thiemens, M.: Impact of preindustrial biomass-burning emissions on the oxidation pathways of tropospheric sulfur and nitrogen, J. Geophys. Res., 109, D08303, doi:10.1029/2003JD004218, 2004.

Alley, R., Finkel, R., Nishizumi, K., Anandakrishnan, A., Shuman, C., Mershon, G., Zielinski, G., and Mayewski, P.A.: Changes in continental and sea-salt atmospheric loadings in central Greenland during the most recent deglaciation: Model-based estimates, J. Glaciol., 41, 503-514, 1995.

Arthern, R.J., Winebrenner, D.P., and Vaughan, D.G.: Antarctic snow accumulation mapped using polarization of 4.3-cm wavelength microwave emission, J. Geophys. Res., 111, doi:10.1029/2004JD005667, 2006.

Barrie, L.A.: Scavenging ratios, wet deposition, and in-cloud oxidation: An application to the oxides of sulphur and nitrogen, J. Geophys. Res., 90, 5789–5799, 1985.

Berhanu, T.A., Savarino, J., Erbland, J., Vicars, W.C., Preunkert, S., Martins, J.F., and Johnson, M.S.: Isotopic effects of nitrate photochemistry in snow: a field study at Dome C, Antarctica, Atmos. Chem. Phys., 15, 11243-11256, doi:10.5194/acp-15-11243-2015, 2015.

Bertler, N., Mayewski, P.A., Aristarain, A., Barrett, P., Becagli, S., Bernardo, R., Bo, S., Xiao, C.,

Curran, M., and Qin, D.: Snow chemistry across Antarctica, Ann. Glaciol., 41, 167-179, 2005.

Blunier, T., Floch, G., Jacobi, H.-W., and Quansah, E.: Isotopic view on nitrate loss in Antarctic surface snow, Geophys. Res. Lett., 32, L13501, doi:10.1029/2005GL023011, 2005.

Brown, S., Ryerson, T., Wollny, A., Brock, C., Peltier, R., Sullivan, A., Weber, R., Dube, W., Trainer, M., and Meagher, J.: Variability in nocturnal nitrogen oxide processing and its role in regional air quality, Science, 311, 67-70, doi:10.1126/science.1120120, 2006.

Burkhart, J.F., Bales, R.C., McConnell, J.R., Hutterli, M.A., and Frey, M.M.: Geographic variability of nitrate deposition and preservation over the Greenland Ice Sheet, J. Geophys. Res., 114, doi:10.1029/2008JD010600, 2009.

Carmagnola, C., Domine, F., Dumont, M., Wright, P., Strellis, B., Bergin, M., Dibb, J., Picard, G., and Morin, S.: Snow spectral albedo at Summit, Greenland: measurements and numerical simulations based on physical and chemical properties of the snowpack, The Cryosphere, 7, 1139-1160, doi:10.5194/tc-7-1139-2013, 2013.

Cook, P., and Roscoe, H.K.: Variability and trends in stratospheric NO_2 in Antarctic summer, and implications for stratospheric NO_y, Atmos. Chem. Phys., 9, 3601-3612, 2009.

Cragin, J., and McGilvary, R., 1995. Can inorganic chemical species volatilize from snow?, in: Tonnessen, K.A., Williams, M.W., Tranter, M. (Eds.), Biogeochemistry of Seasonally Snow-Covered Catchments. IAHS Press, Wallingford, UK, pp. 11-16.

Das, I., Bell, R.E., Scambos, T.A., Wolovick, M., Creyts, T.T., Studinger, M., Frearson, N., Nicolas, J.P., Lenaerts, J.T., and van den Broeke, M.R.: Influence of persistent wind scour on the surface mass balance of Antarctica, Nat. Genet, 6, 367-371, doi:10.1038/NGEO1766, 2013.

Ding, M., Xiao, C., Jin, B., Ren, J., Qin, D., and Sun, W.: Distribution of $\delta^{18}O$ in surface snow along a transect from Zhongshan Station to Dome A, East Antarctica, Chin. Sci. Bull., 55, 2709-2714, doi:10.1007/s11434-010-3179-3, 2010.

Ding, M., Xiao, C., Li, Y., Ren, J., Hou, S., Jin, B., and Sun, B.: Spatial variability of surface mass balance along a traverse route from Zhongshan station to Dome A, Antarctica, J. Glaciol., 57, 658-666, 2011.

Erbland, J., Savarino, J., Morin, S., France, J.L., Frey, M.M., and King, M.D.: Air-snow transfer of nitrate on the East Antarctic plateau -Part 2: An isotopic model for the interpretation of deep ice-core records, Atmos. Chem. Phys., 15, 12079–12113, doi:10.5194/acp-15-12079-2015, 2015.

Erbland, J., Vicars, W., Savarino, J., Morin, S., Frey, M., Frosini, D., Vince, E., and Martins, J.: Air-snow transfer of nitrate on the East Antarctic Plateau - Part 1: Isotopic evidence for a photolytically driven dynamic equilibrium in summer, Atmos. Chem. Phys., 13, 6403-6419, doi:10.5194/acp-13-6403-2013, 2013.

Felix, J.D., and Elliott, E.M.: The agricultural history of human - nitrogen interactions as recorded in ice core δ15N - NO3−, Geophys. Res. Lett., 40, 1642-1646, doi:10.1002/grl.50209, 2013.

Fibiger, D.L., Hastings, M.G., Dibb, J.E., and Huey, L.G.: The preservation of atmospheric nitrate in snow at Summit, Greenland, Geophys. Res. Lett., 40, 3484-3489, doi:10.1002/grl.50659, 2013.

Fischer, H., and Wagenbach, D.: Large-scale spatial trends in recent firn chemistry along an east-west transect through central Greenland, Atmos. Environ., 30, 3227-3238, 1996.

Frey, M.M., Savarino, J., Morin, S., Erbland, J., and Martins, J.: Photolysis imprint in the nitrate stable isotope signal in snow and atmosphere of East Antarctica and implications for reactive nitrogen cycling, Atmos. Chem. Phys., 9, 8681-8696, 2009.

Geng, L., Alexander, B., Cole-Dai, J., Steig, E.J., Savarino, J., Sofen, E.D., and Schauer, A.J.: Nitrogen

isotopes in ice core nitrate linked to anthropogenic atmospheric acidity change, Proc. Natl. Acad. Sci., 111, 5808-5812, doi:10.1073/pnas.1319441111, 2014.

Geng, L., Murray, L.T., Mickley, L.J., Lin, P., Fu, Q., Schauer, A.J., and Alexander, B.: Isotopic evidence of multiple controls on atmospheric oxidants over climate transitions, Nature, 546, 133-136, doi:10.1038/nature22340, 2017.

Goodwin, I., De Angelis, M., Pook, M., and Young, N.: Snow accumulation variability in Wilkes Land, East Antarctica, and the relationship to atmospheric ridging in the 130°-170° E region since 1930, J. Geophys. Res., 108, doi:10.1029/2002JD002995 2003.

Grannas, A., Jones, A.E., Dibb, J., Ammann, M., Anastasio, C., Beine, H., Bergin, M., Bottenheim, J., Boxe, C., and Carver, G.: An overview of snow photochemistry: evidence, mechanisms and impacts, Atmos. Chem. Phys., 7, 4329-4373, 2007.

Hara, K., Nakazawa, F., Fujita, S., Fukui, K., Enomoto, H., and Sugiyama, S.: Horizontal distributions of aerosol constituents and their mixing states in Antarctica during the JASE traverse, Atmos. Chem. Phys., 14, 10211-10230, doi:10.5194/acp-14-10211-2014, 2014.

Hara, K., Osada, K., Kido, M., Matsunaga, K., Iwasaka, Y., Hashida, G., and Yamanouchi, T.: Variations of constituents of individual sea-salt particles at Syowa station, Antarctica, Tellus B, 57, 230-246, 2005.

Hastings, M.G., Jarvis, J.C., and Steig, E.J.: Anthropogenic impacts on nitrogen isotopes of ice-core nitrate, Science, 324, 1288-1288, doi:10.1126/science.1170510, 2009.

Hastings, M.G., Steig, E., and Sigman, D.: Seasonal variations in N and O isotopes of nitrate in snow at Summit, Greenland: Implications for the study of nitrate in snow and ice cores, J. Geophys. Res., 109, D20306, doi:10.1029/2004JD004991, 2004.

Holland, P.R., Bruneau, N., Enright, C., Losch, M., Kurtz, N.T., and Kwok, R.: Modeled Trends in Antarctic Sea Ice Thickness, J. Climate, 27, 3784-3801, doi:10.1175/JCLI-D-13-00301.1, 2014.

Hou, S., Li, Y., Xiao, C., and Ren, J.: Recent accumulation rate at Dome A, Antarctica, Chin. Sci. Bull., 52, 428-431, 2007.

Jones, A.E., Weller, R., Minikin, A., Wolff, E.W., Sturges, W.T., Mcintyre, H.P., Leonard, S.R., Schrems, O., and Bauguitte, S.: Oxidized nitrogen chemistry and speciation in the Antarctic troposphere, J. Geophys. Res., 1042, 21355-21366, 1999.

Kasper-Giebl, A., Kalina, M.F., and Puxbaum, H.: Scavenging ratios for sulfate, ammonium and nitrate determined at Mt. Sonnblick (3106m a.s.l.), Atmos. Environ., 33, 895-906, 1999.

Laluraj, C., Thamban, M., Naik, S., Redkar, B., Chaturvedi, A., and Ravindra, R.: Nitrate records of a shallow ice core from East Antarctica: Atmospheric processes, preservation and climatic implications, The Holocene, 21, 351-356, doi:10.1177/0959683610374886, 2010.

Lee, H.-M., Henze, D.K., Alexander, B., and Murray, L.T.: Investigating the sensitivity of surface-level nitrate seasonality in Antarctica to primary sources using a global model, Atmos. Environ., 89, 757-767, doi:10.1016/j.atmosenv.2014.03.003, 2014.

Legrand, M., and Kirchner, S.: Origins and variations of nitrate in South Polar precipitation, J. Geophys. Res., 95, 3493-3507 1990.

Legrand, M., and Mayewski, P.A.: Glaciochemistry of polar ice cores: a review, Rev. Geophys., 35, 219-243, 1997.

Legrand, M.R., and Delmas, R.J.: Soluble impurities in four Antarctic ice cores over the last 30,000 years, Ann. Glaciol., 10, 116-120, 1988.

Li, C., Ren, J., Qin, D., Xiao, C., Hou, S., Li, Y., and Ding, M.: Factors controlling the nitrate in the

DT-401 ice core in eastern Antarctica, Sci. China Ser. D, doi:10.1007/s11430-012-4557-2, 2013.

Li, Y., Cole-Dai, J., and Zhou, L.: Glaciochemical evidence in an East Antarctica ice core of a recent (AD 1450-1850) neoglacial episode, J. Geophys. Res., 114, doi:10.1029/2008JD011091, 2009.

Li, Z., Zhang, M., Qin, D., Xiao, C., Tian, L., Kang, J., and Li, J.: The seasonal variations of $\delta^{18}O$, Cl^-, Na^+, NO_3^- and Ca^{2+} in the snow and firn recovered from Princess Elizabeth Land, Antarctica, Chin. Sci. Bull., 44, 2270-2273, 1999.

Liss, P.S., Chuck, A.L., Turner, S.M., and Watson, A.J.: Air-sea gas exchange in Antarctic waters, Antarct. Sci., 16, 517-529, doi:10.1017/S0954102004002299, 2004.

Ma, Y., Bian, L., Xiao, C., Allison, I., and Zhou, X.: Near surface climate of the traverse route from Zhongshan Station to Dome A, East Antarctica, Antarct. Sci., 22, 443-459, doi:10.1017/S0954102010000209, 2010.

Marion, G., Farren, R., and Komrowski, A.: Alternative pathways for seawater freezing, Cold Reg. Sci. Technol., 29, 259-266, 1999.

Mayewski, P.A., and Legrand, M.R.: Recent increase in nitrate concentration of Antarctic snow, Nature, 346, 258-260, 1990.

McCabe, J.R., Thiemens, M.H., and Savarino, J.: A record of ozone variability in South Pole Antarctic snow: Role of nitrate oxygen isotopes, J. Geophys. Res., 112, D12303, doi:10.1029/2006JD007822, 2007.

Mosley-Thompson, E., Dai, J., Thompson, L., Grootes, P., Arbogast, J.K., and Paskievitch, J.: Glaciological studies at Siple Station (Antarctica): potential ice-core paleoclimatic record, J. Glaciol., 37, 11-22, 1991.

Mulvaney, R., and Wolff, E.: Spatial variability of the major chemistry of the Antarctic ice sheet, Ann. Glaciol., 20, 440-447, 1994.

Parish, T.R., and Bromwich, D.H.: Reexamination of the near-surface airflow over the Antarctic continent and implications on atmospheric circulations at high southern latitudes, Mon. Weather. Rev., 135, 1961-1973, doi:10.1175/MWR3374.1, 2007.

Pasteris, D., McConnell, J.R., Edwards, R., Isaksson, E., and Albert, M.R.: Acidity decline in Antarctic ice cores during the Little Ice Age linked to changes in atmospheric nitrate and sea salt concentrations, J. Geophys. Res., 119, 5640-5652, doi:10.1002/2013JD020377, 2014.

Qin, D., Zeller, E.J., and Dreschhoff, G.A.: The distribution of nitrate content in the surface snow of the Antarctic Ice Sheet along the route of the 1990 International Trans-Antarctica Expedition, J. Geophys. Res., 97, 6277-6284, 1992.

Röthlisberger, R., Hutterli, M.A., Sommer, S., Wolff, E.W., and Mulvaney, R.: Factors controlling nitrate in ice cores: Evidence from the Dome C deep ice core, J. Geophys. Res., 105, 20565-20572, 2000.

Röthlisberger, R., Mulvaney, R., Wolff, E.W., Hutterli, M.A., Bigler, M., De Angelis, M., Hansson, M.E., Steffensen, J.P., and Udisti, R.: Limited dechlorination of sea-salt aerosols during the last glacial period: Evidence from the European Project for Ice Coring in Antarctica (EPICA) Dome C ice core, J. Geophys. Res., 108, 4526, doi:4510.1029/2003JD003604, 2003.

Russell, A., McGregor, G., and Marshall, G.: 340 years of atmospheric circulation characteristics reconstructed from an eastern Antarctic Peninsula ice core, Geophys. Res. Lett., 33, L08702, doi:08710.01029/02006GL025899, 2006.

Russell, A., Mcgregor, G.R., and Marshall, G.J.: An examination of the precipitation delivery mechanisms for Dolleman Island, eastern Antarctic Peninsula, Tellus Series A-dynamic

Meteorology & Oceanography, 56, 501–513, 2004.

Sato, K., Takenaka, N., Bandow, H., and Maeda, Y.: Evaporation loss of dissolved volatile substances from ice surfaces, J. Phys. Chem., 112, 7600-7607, doi:10.1021/jp075551r, 2008.

Savarino, J., Kaiser, J., Morin, S., Sigman, D.M., and Thiemens, M.H.: Nitrogen and oxygen isotopic constraints on the origin of atmospheric nitrate in coastal Antarctica, Atmos. Chem. Phys., 7, 1925-1945, 2007.

Seinfeld, J.H., and Pandis, S.N., 1997. Atmospheric Chemistry and Physics: From Air Pollution to Climate Change, 2nd ed. Wiley, New York.

Shi, G., Buffen, A.M., Hastings, M.G., Li, C., Ma, H., Li, Y., Sun, B., An, C., and Jiang, S.: Investigation of post-depositional processing of nitrate in East Antarctic snow: isotopic constraints on photolytic loss, re-oxidation, and source inputs, Atmos. Chem. Phys., 15, 9435–9453, doi:10.5194/acp-15-9435-2015, 2015.

Shi, G., Li, Y., Jiang, S., An, C., Ma, H., Sun, B., and Wang, Y.: Large-scale spatial variability of major ions in the atmospheric wet deposition along the China Antarctica transect (31^{o} N~ 69^{o} S), Tellus B, 64, 17134, doi:10.3402/tellusb.v64i0.17134, 2012.

Traversi, R., Becagli, S., Brogioni, M., Caiazzo, L., Ciardini, V., Giardi, F., Legrand, M., Macelloni, G., Petkov, B., Preunkert, S., Scarchilli, C., Severi, M., Vitale, V., and Udisti, R.: Multi-year record of atmospheric and snow surface nitrate in the central Antarctic plateau, Chemosphere, 172, 341-354, doi:10.1016/j.chemosphere.2016.12.143, 2017.

Traversi, R., Becagli, S., Castellano, E., Cerri, O., Morganti, A., Severi, M., and Udisti, R.: Study of Dome C site (East Antartica) variability by comparing chemical stratigraphies, Microchem. J., 92, 7-14, doi:10.1016/j.microc.2008.08.007, 2009.

Traversi, R., Usoskin, I., Solanki, S., Becagli, S., Frezzotti, M., Severi, M., Stenni, B., and Udisti, R.: Nitrate in Polar Ice: A New Tracer of Solar Variability, Sol. Phys., 280, 237-254, 2012.

Wagenbach, D., Graf, V., Minikin, A., Trefzer, U., Kipfstuhl, J., Oerter, H., and Blindow, N.: Reconnaissance of chemical and isotopic firn properties on top of Berkner Island, Antarctica, Ann. Glaciol., 20, 307-312, 1994.

Wagenbach, D., Legrand, M., Fischer, H., Pichlmayer, F., and Wolff, E.W.: Atmospheric near-surface nitrate at coastal Antarctic sites, J. Geophys. Res., 103, 11007-11020, 1998.

Warren, S.G., Brandt, R.E., and Grenfell, T.C.: Visible and near-ultraviolet absorption spectrum of ice from transmission of solar radiation into snow, Appl. Optics, 45, 5320-5334, 2006.

Witherow, R.A., Lyons, W.B., Bertler, N.A., Welch, K.A., Mayewski, P.A., Sneed, S.B., Nylen, T., Handley, M.J., and Fountain, A.: The aeolian flux of calcium, chloride and nitrate to the McMurdo Dry Valleys landscape: evidence from snow pit analysis, Antarct. Sci., 18, 497-505, doi:10.1017/S095410200600054X, 2006.

Wolff, E.W.: Nitrate in polar ice. In Delmas R J ed. Ice core studies of global biogeochemical cycles, 195-224. Berlin, Springer-Verlag. 1995 1995.

Wolff, E.W., Jones, A.E., Bauguitte, S.-B., and Salmon, R.A.: The interpretation of spikes and trends in concentration of nitrate in polar ice cores, based on evidence from snow and atmospheric measurements, Atmos. Chem. Phys., 8, 5627-5634, 2008.

Xiao, C., Mayewski, P.A., Qin, D., Li, Z., Zhang, M., and Yan, Y.: Sea level pressure variability over the southern Indian Ocean inferred from a glaciochemical record in Princess Elizabeth Land, east Antarctica, J. Geophys. Res., 109, doi:10.1029/2003JD004065, 2004.

Zatko, M., Grenfell, T., Alexander, B., Doherty, S., Thomas, J., and Yang, X.: The influence of snow

grain size and impurities on the vertical profiles of actinic flux and associated NO_x emissions on the Antarctic and Greenland ice sheets, Atmos. Chem. Phys., 13, 3547-3567, doi:10.5194/acp-13-3547-2013, 2013.

Zatko, M.C., Geng, L., Alexander, B., Sofen, E.D., and Klein, K.: The impact of snow nitrate photolysis on boundary layer chemistry and the recycling and redistribution of reactive nitrogen across Antarctica and Greenland in a global chemical transport model, Atmos. Chem. Phys., 16, 2819-2842, doi:10.5194/acp-16-2819-2016, 2016.

Zeller, E.J., Dreschhoff, G.A., and Laird, C.M.: Nitrate flux on the Ross Ice Shelf, Antarctica and its relation to solar cosmic rays, Geophys. Res. Lett., 13, 1264-1267, 1986.

The Cryosphere Discuss., https://doi.org/10.5194/tc-2017-227
Manuscript under review for journal The Cryosphere
Discussion started: 20 October 2017

716 **Table 1.** Snowpit information on the traverse from coastal Zhongshan station to Dome A, East
717 Antarctica.

Snowpit No.	Latitude, °	Longitude, °	Elevation, m	Distance to coast, km	Annual snow accumulation, kg m^{-2} a^{-1} 1)	Depth, cm	Sampling resolution, cm	Sampling year
SP1	-70.52	76.83	1613	132	193.2	150	5.0	2010/2011
SP2	-71.13	77.31	2037	200	172.0	150	3.0	2012/2013
SP3	-71.81	77.89	2295	283	99.4	200	5.0	2012/2013
SP4	-72.73	77.45	2489	387	98.3	200	5.0	2012/2013
SP5	-73.40	77.00	2545	452	90.7	200	5.0	2012/2013
SP6	-73.86	76.98	2627	514	24.6	300	2.5	2012/2013
SP7	-74.50	77.03	2696	585	29.2	100	2.0	2012/2013
SP8	-74.65	77.01	2734	602	80.2	180	2.0	2010/2011
SP9	-76.29	77.03	2843	787	54.8	200	2.0	2012/2013
SP10	-76.54	77.02	2815	814	100.7	240	3.0	2010/2011
SP11	-77.13	76.98	2928	879	81.2	200	2.5	2012/2013
SP12	-77.26	76.96	2962	893	83.4	265	5.0	2009/2010
SP13	-77.91	77.13	3154	968	33.3	200	2.0	2012/2013
SP14	-78.34	77.00	3368	1015	87.6	216	3.0	2010/2011
SP15	-78.35	77.00	3366	1017	70.0	162	2.0	2009/2010
SP16	-79.02	76.98	3738	1092	25.4	200	2.5	2012/2013
SP17	-79.65	77.21	3969	1162	46.2	130	2.0	2010/2011
SP18	-80.40	77.15	4093	1250	24.2	300	2.0	2010/2011
SP19	-80.41	77.11	4092	1254	23.7	300	1.0	2009/2010
SP20	-80.42	77.12	4093	1256	23.5	300	2.5	2012/2013
Core 1[2)]	-70.83	77.08	1850	168	127.0	-	-	1996/1997
Core 2[3)]	-76.53	77.03	2814	810	101.0	-	-	1998/1999

718 1) Annual snow accumulation rate is obtained from the field bamboo stick measurements (2009 - 2013),
719 updated from the report (Ding et al., 2011). Note that snow accumulation rate at the two ice core sites
720 are derived from ice core measurements.
721 2) Core 1, ice core data of previous report (Li et al., 1999; Xiao et al., 2004).
722 3) Core 2, ice core data of previous report (Li et al., 2009).
723

The Cryosphere Discuss., https://doi.org/10.5194/tc-2017-227
Manuscript under review for journal The Cryosphere
Discussion started: 20 October 2017

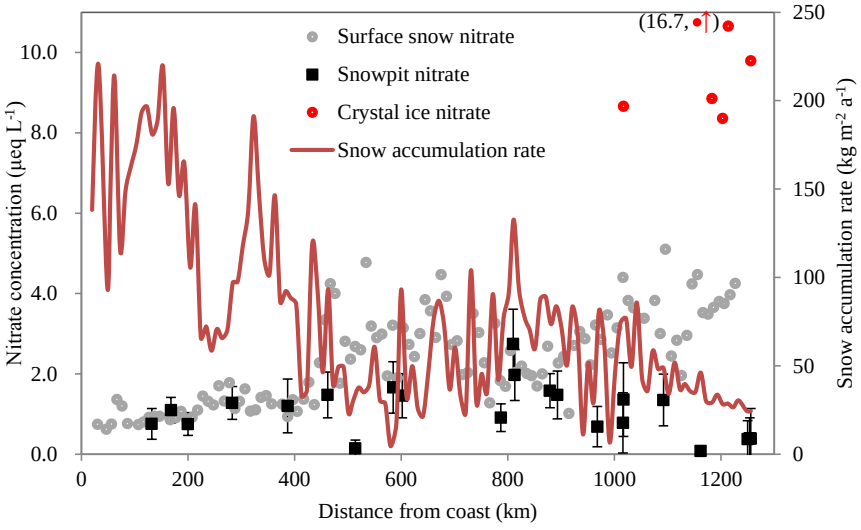

Figure 1. Concentrations of NO_3^- in surface snow, crystal ice and snowpits, with error bars representing one standard deviation of NO_3^- (1σ) for individual snowpits. Also shown is the annual snow accumulation rate on the traverse (red solid line; based on Ding et al. (2011)). Note that NO_3^- concentration in one crystal ice sample (red dot), 16.7 μeq L^{-1} in the parentheses, is higher than the maximum value of the primary *y*-axis (NO_3^- concentration).

The Cryosphere Discuss., https://doi.org/10.5194/tc-2017-227
Manuscript under review for journal The Cryosphere
Discussion started: 20 October 2017

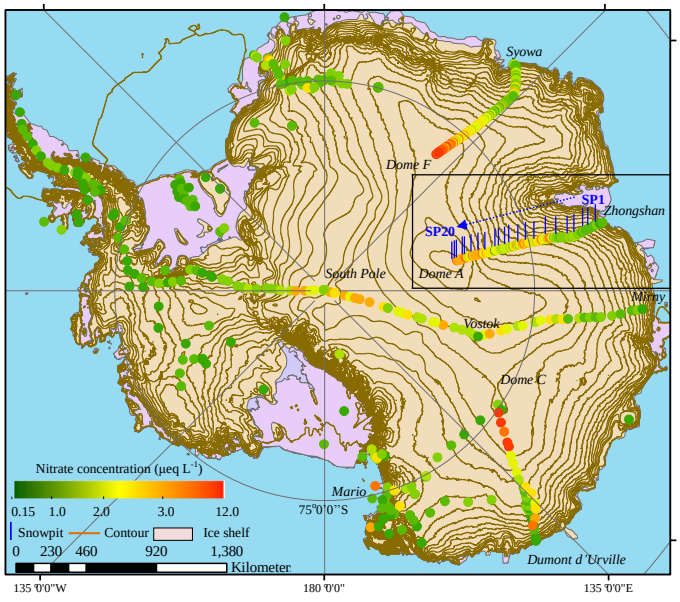

Figure 2. Concentrations of NO_3^- in surface snow across Antarctica. Note that the values of crystal ice around Dome A were not included. The data of DDU to Dome C is from Frey et al. (2009). The other surface snow NO_3^- concentrations are from the compiled data (Bertler et al., 2005)and references therein). Also illustrated are the locations of snowpits on the traverse route from Zhongshan to Dome A in this study (SP1 to SP20, solid blue line; Table 1).

The Cryosphere Discuss., https://doi.org/10.5194/tc-2017-227
Manuscript under review for journal The Cryosphere
Discussion started: 20 October 2017

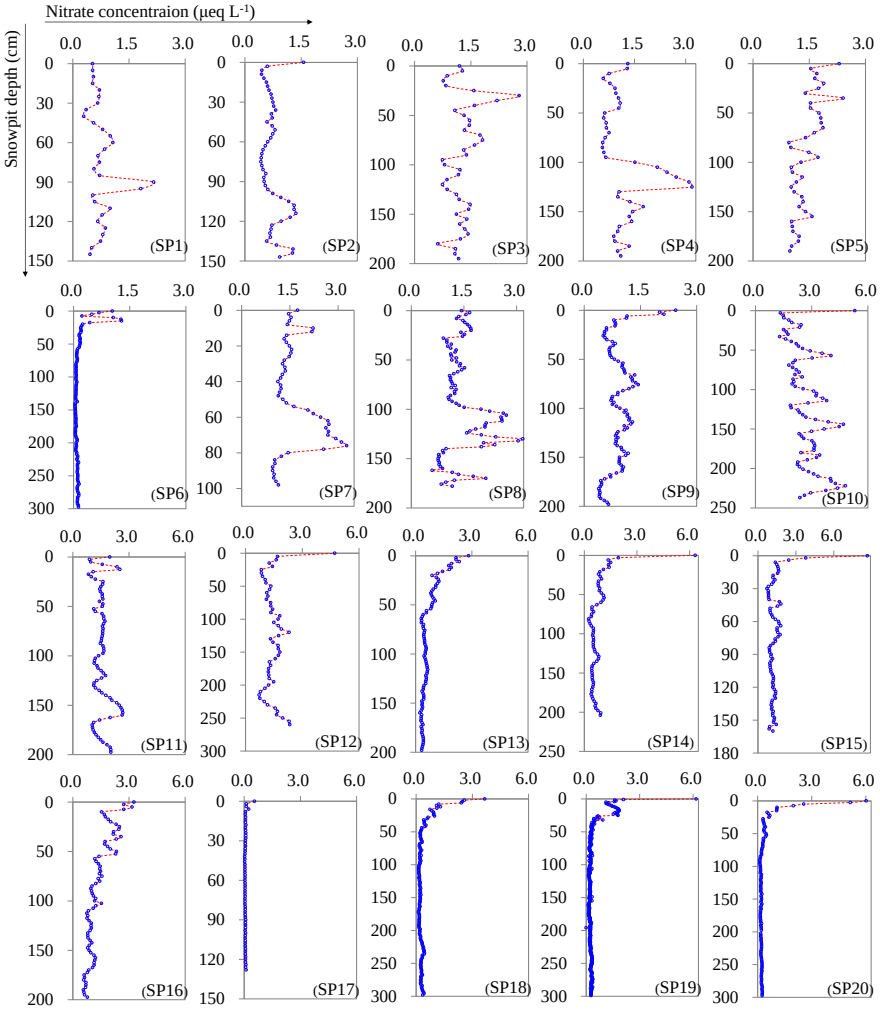

Figure 3. The full profiles of NO_3^- concentrations for snowpits collected on the traverse from the coast to Dome A, East Antarctica (SP1 is closest the coast; SP20 the furthest inland; see Figure 2). The details on sampling of the snowpits refer to Table 1. Note that the scales of x-axes for the snowpits SP1 – SP9 and SP10 – SP 20 are different.

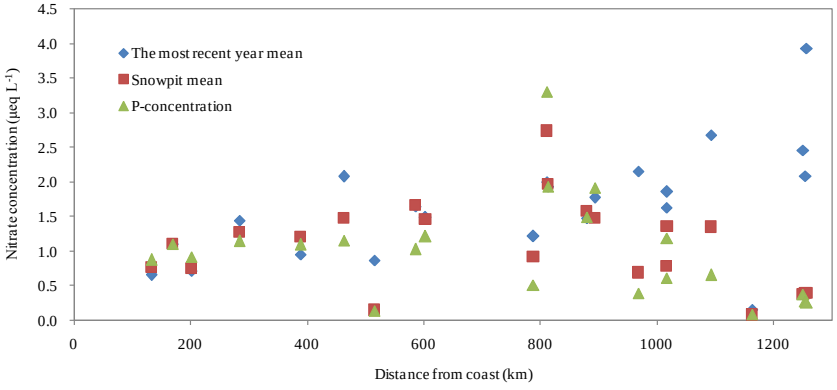

745

746 **Figure 4.** Mean concentrations of NO_3^- for the entire snowpit (snowpit mean, in square), the uppermost
747 layer covering one-year snow accumulation (the most recent year mean, in diamond) and the bottom
748 layer covering a full annual cycle of deposition (p-concentration, in triangle).

749

The Cryosphere Discuss., https://doi.org/10.5194/tc-2017-227
Manuscript under review for journal The Cryosphere
Discussion started: 20 October 2017

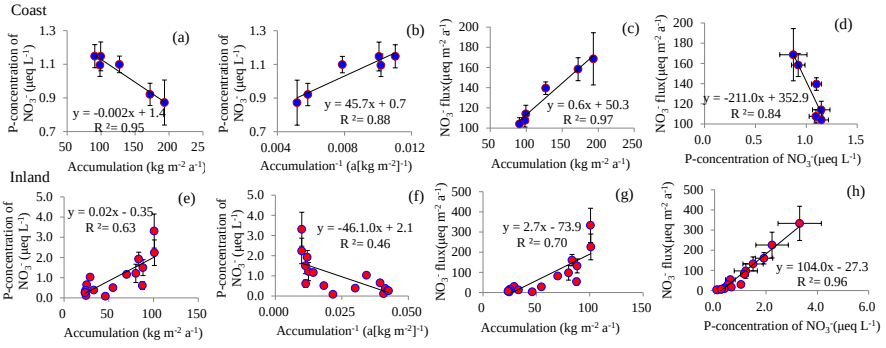

Figure 5. The relationship among snow accumulation rate, the concentration, and flux of NO_3^- in coastal (top row, (a), (b), (c) and (d)) and inland (bottom row, (e), (f), (g) and (h)) Antarctica. The flux values are the product of p-concentration of NO_3^- (for details see main text) and snow accumulation rate, namely the archived flux. Least squares regressions are noted with solid lines and are significant at $p < 0.01$. Error bars represent one standard deviation (1σ).

The Cryosphere Discuss., https://doi.org/10.5194/tc-2017-227
Manuscript under review for journal The Cryosphere
Discussion started: 20 October 2017

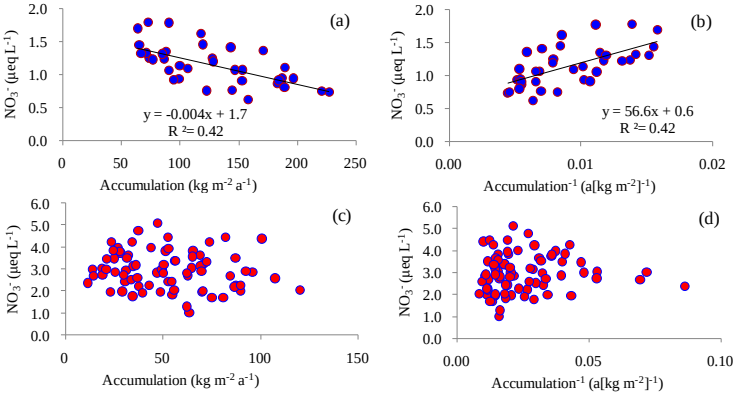

Figure 6. The relationship between NO_3^- concentration and snow accumulation rate in surface snow at the coast (top row, (a) and (b)) and inland (bottom row, (c) and (d)) Antarctica. Least squares regressions are noted with solid line and are significant at $p < 0.01$.

The Cryosphere Discuss., https://doi.org/10.5194/tc-2017-227
Manuscript under review for journal The Cryosphere
Discussion started: 20 October 2017

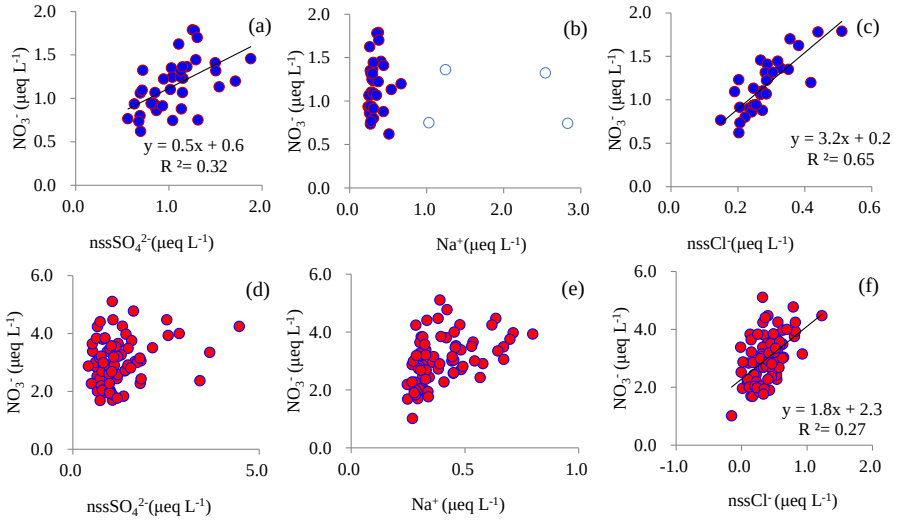

Figure 7. Relationships between NO_3^- and major ions in surface snow in coastal (top row, (a), (b) and (c)) and inland (bottom row, (d), (e) and (f)) Antarctica. Least squares regressions are noted with solid line and are significant at $p < 0.01$. The 4 samples with high Na^+ concentrations are denoted by blue open circles (b), the same as those in Figure 8 (the blue open circles). Note that the 4 samples were excluded in the plot of NO_3^- vs. $nssCl^-$ (c).

The Cryosphere Discuss., https://doi.org/10.5194/tc-2017-227
Manuscript under review for journal The Cryosphere
Discussion started: 20 October 2017

771

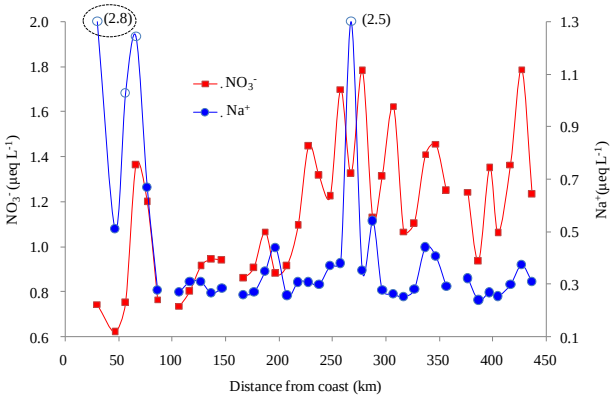

772

773 **Figure 8.** Concentrations of NO_3^- and Na^+ in surface snow samples on the coast. Four samples with
774 high Na^+ concentrations are denoted by open circles, corresponding to those in Fig. 7b. Note that Na^+
775 concentrations in two samples, 2.5 and 2.8 μeq L^{-1} in parentheses, are above the maximum value of the
776 secondary *y*-axis (Na^+ concentration). The sample in the dashed ellipse, with Na^+ concentration of 2.8
777 μeq L^{-1}, is the fresh snowfall.

778